


Investigation on Tenofovir Removal from Water by Electro-Fenton Process: Optimization of the Mineralization using Box-Behnken Design

Lys Carelle Motue Waffo ^{1,2}, Jean Marie Dangwang Dikdim ³, Guy Bertrand Noumi ², Joseph Marie Sieliechi ⁴, Aicha Guessous ¹, Fouad Echerfaoui ⁵, Miloud El Karbane ⁵, Ismail Warad ⁶, Abdelkader Zarrouk ^{1,*}, Ghizlan Kaichouh ^{1,*} 

¹ Laboratory of Materials, Nanotechnology, and Environment, Faculty of Sciences, Mohammed V University in Rabat, P.O. Box 1014, Rabat, Morocco

² Department of Chemistry, Faculty of Science, University of Ngaoundere P.O. Box: 454 Ngaoundere, Cameroon

³ Department of Chemistry, Faculty of Science, University of Maroua, P.O. Box: 814 Maroua, Cameroon

⁴ Department of Applied Chemistry, National School of Agro-Industrial Science, University of Ngaoundere, P.O. Box: 455 Ngaoundere, Cameroon

⁵ Laboratory of Analytical Chemistry and Bromatology, Faculty of Medicine and Pharmacy of Rabat, University Mohammed V, Rabat, Morocco

⁶ Department of Chemistry, AN-Najah National University, P.O. Box 7, Nablus, Palestine

* Correspondence: azarrouk@gmail.com (A.Z.); g.kaichouh@gmail.com (G.K.);

Scopus Author ID 36125763200

Received: 17.09.2022; Accepted: 6.11.2022; Published: 4.02.2023

Abstract: The release of emerging pollutants, such as pharmaceutical compounds, into the environment degrades its quality seriously. Tenofovir (TEN) is a drug used to fight viral illnesses. It is non-biodegradable and remains in the environment, and causes the pollution of surface water and groundwater. This work is then focused on optimizing the mineralization of TEN in an aqueous medium by the Electro-Fenton process. The influences of some experimental parameters were studied during the degradation and mineralization of TEN versus time. The concentration decay of TEN and the mineralization were followed by HPLC and COD measures, respectively. The biodegradability was also monitored by determining the biological oxygen demand (BOD₅). The optimization of the COD removal was studied by the surface response methodology, following the Box Behnken Design (BBD). The results obtained showed a complete degradation (100%) of the TEN after 20 minutes. The kinetic study of the degradation of the TEN has shown that it obeys the pseudo-first-order law whose optimal apparent constant (0.254 min⁻¹) was obtained at 300 mA. The biodegradability BOD₅/COD ratio increased from 0.2 to 11 after 5 h of treatment, which permitted us to see the importance of coupling Biodegradation/Electro-Fenton for TEN removals. The total mineralization of TEN was obtained at satisfactory optimal conditions of 282 mA and 0.1 mM for the initial concentration of TEN after 164 minutes of electrolysis. This finding provides a significant contribution to emerging pollutants removal from aqueous media by the EF process.

Keywords: Tenofovir; Electro-Fenton; degradation; hydroxyl radical; response surface methodology.

© 2023 by the authors. This article is an open-access article distributed under the terms and conditions of the Creative Commons Attribution (CC BY) license (<https://creativecommons.org/licenses/by/4.0/>).

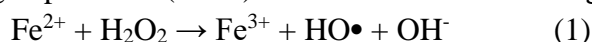
1. Introduction

Emerging pollutants are all chemicals used in everyday life and industrial, agricultural, and health applications. These are pharmaceutical substances, industrial and domestic chemical products, and degradation products (of pharmaceutical, industrial, and domestic products). All

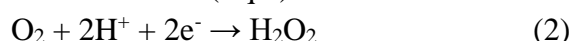
these products mainly end up in wastewater after use. High concentrations of emerging pollutants have been found in birds and marine mammals [1–5]. Therefore, due to the biotransformation capacity of these compounds, the degradation by-products can generally be more harmful than the parent substances [6]. Most of the time, environmental waters are the main final destination of drugs. This creates a major pollution problem because the real information on their toxicity on humans and environmental impacts is well not known.

The number of people with HIV has been steadily increasing over the years. In 2010, we estimated the population living with HIV and hepatitis B to be over 34 million people worldwide [7]. This number increased considerably in 2015, and it reached 39.5 million people in the world [8]. Tenofovir (TEN) is an acyclic nucleotide analog of adenosine used in combination with other agents in the treatment of human immunodeficiency virus (HIV) and as monotherapy in hepatitis B virus (HBV) infection [7,9,10]. This consumption is estimated at 5.94 tons per day worldwide, but the human body ingests only 1% of this consumption, and 99% is rejected in the form of urine and excrement [11]. In addition, the high production of Tenofovir by the pharmaceutical industries also induces a significant discharge of wastewater into the environment, which poses a significant risk for environmental pollution and human health [12]. It has been detected at low concentrations (145-243 ng/L) in South African surface waters [13] and (2.35 ng/L) in surface waters globally [11]. Previous work has also shown that TEN is a non-biodegradable molecule found in aquatic plants and animals due to its presence in surface and ground waters [14]. It is, therefore important to find a treatment method to eliminate it from the water before releasing it into the environment.

Conventional physicochemical water treatment methods, membrane filtration, and adsorption contribute to transferring the pollutants from the liquid to the solid phase. However, biological processes have proven ineffective in eliminating most drugs from their persistence and also from the fact that they are very dangerous for microorganisms [11,12]. Consequently, research was intensively concentrated on finding alternative efficient treatment methods for organic pollutant elimination. Electrochemical Advanced oxidation processes (EAOPs) like Electro-Fenton (EP) and Electro-Oxidation (EO) have particularly received great interest in recent years because they allow the mineralization of recalcitrant compounds into inorganic ions, CO₂ and H₂O. Compared to EO, the Electro-Fenton (EF) Process, based on the in situ electrochemical formation of hydroxyl radicals (HO•), has been a good technique for the removal of recalcitrant and harmful organic pollutants from aqueous media [13–22]. HO• radicals are very powerful, non-selective, and highly reactive oxidants. In the EF process, HO• radicals are in situ produced by electrochemically assisted Fenton reaction involving hydrogen peroxide (H₂O₂) and ferrous ions according to the following reaction (Eq 1):



The generation of hydrogen peroxide was obtained by the reduction of dissolved oxygen in the solution (Eq 2).



Regarding the ferrous ions, they are added in the medium as a catalyst, and they are also provided the simultaneous reduction of ferric ions (Eq 3).



The attractive point of the EF process is related to the in situ continuous generation of H₂O₂. Also, the EF process is simple and easy to operate, making it a promising method for eliminating toxic compounds. The efficiency of organic compounds degradation by EF process is influenced by various experimental parameters such as pollutant concentration, catalyst

concentration, and current intensity. However, it should be noted that the main criterion of a good AOP is achieving a complete mineralization step at a low cost. In the case of EF process, this economic aspect was mainly focused both on little consumption of reagents and electric energy. In this context, to optimize the efficiency of the process, some parameters were usually submitted to the Response Surface Methodology (RSM) approach in the literature [23–26]. Generally, we use RSM, one of the most used tools to model and study multivariate systems to generate a response surface [31]. Box-Behnken Design (BBD) was adopted in this work because it reduces the number of experiments and the cost of reagent [27,28].

In this work, the evaluation of the effect of operational parameters (the intensity of the current, amount of Fe^{2+} , and initial TEN concentration) influencing the EF process during the kinetic degradation of the TEN was investigated. Secondly, the evolution of the biodegradability of the TEN solutions was followed based on the BOD5/COD ratio after having carried out the coupling EF and biological treatment. Finally, the optimization of certain parameters (the current intensity, the initial concentration of the TEN, and electrolysis time) was investigated by applying the BBD.

2. Material and Methods

2.1. Chemical and reagent.

The industry pharmaceutical Laboratory located in Rabat (Morocco) has provided us with Tenofovir ($\text{C}_9\text{H}_{14}\text{N}_5\text{O}_4\text{P}$) (purity > 98%). Figure 1 represents the chemical structure of TEN. Potassium dichromate (99%) and mercuric sulfate were provided by Panreac Quimica and Hach Lange (Europe, Belgium), respectively, and were supplied by Sigma-Aldrich. Ferrous sulfate ($\text{FeSO}_4 \cdot 7\text{H}_2\text{O}$) and sulfuric acid H_2SO_4 (96%) were purchased from Shanghai chemicals (Shanghai, China) and Sigma-Aldrich (Saint-Quentin Fallavier, France). We prepared all the test solutions with an ultrapure water Milli-Q (Millipore, resistivity > 18 M Ω cm).

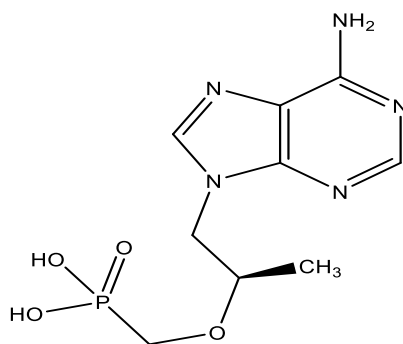


Figure 1. TEN chemical structure

2.2. Electro-Fenton degradation procedure.

Degradation of the TEN by the electro-Fenton process was carried out in an undivided electrochemical cell (6 cm diameter and 250 Ml capacity). The working electrode consists of carbon felt (Carbon Lorraine, (6 × 5 × 0.5 cm), while the anode is 2.5 cm in diameter and 2 cm high (platinum foil). The electrolysis experiments were carried out using a potentiostat galvanostat (Volta Lab, PGZ 100) for the current supply. All working solutions were firstly saturated by bubbling with oxygen contained in a compressed air tank for 10 min. The ionic strength was maintained by adding Na_2SO_4 (0.05 M) as a supporting electrolyte. The iron sulfate ($\text{FeSO}_4 \cdot 7\text{H}_2\text{O}$) catalyzing the Fenton reaction was added to the reaction medium before

the electrolysis. The medium was acidified with sulfuric acid H₂SO₄ (up to a pH between 2.8 and 3) to avoid the precipitation of ferric ions as hydroxides [33]. During all the experiments, the test solutions were maintained under stirring at room temperature, and 2.5 mL was withdrawn at an interval value of 5 min for analysis.

2.3. Analytical techniques

2.3.1. High-performance liquid chromatography (HPLC).

The concentration of TEN was determined by reversed-phase HPLC. The analytical instrument was a system DIONEX UltiMate 3000 equipped with a column C18 (250 × 4.6) mm × 5 μm (Kromasil) and PDA detector (Photodiode Array Detection). The volume injection was 50 μL with a flow rate of 1 mL/min. The mobile phase was a mixture of phosphate buffered/Methanol (70/30) at pH = 5. The chromatograms of the TEN molecules were obtained at 254 nm.

2.3.2. Chemical oxygen demand (COD).

Chemical oxygen demand (COD) was measured using the potassium dichromate assay method. It consisted in oxidizing our samples with potassium dichromate and mercury sulfate in an acid medium. Then we incubate for 2 hours at 150 °C. Finally, we carried out the reading thanks to the colorimetric with a DR/125 spectrophotometer (Hach Company, USA).

2.3.3. Biological oxygen demand (BOD) measurements.

To evaluate the biodegradability of the solution during electrolysis, we measured the biological oxygen demand (BOD). The activated sludge was obtained from a wastewater treatment plant located in Rabat city. The procedure for determining BOD₅ was applied on blank and test solutions according to the previously described method [28,30,31].

2.4. The instantaneous current efficiency (% ICE).

The instantaneous current efficiency (ICE) represents the quantity of current capable of oxidizing the organic compounds and was calculated according to Eq. (4)

$$ICE = \frac{(DCO_0 - DCO_t) \times F \times V}{8 \times I \times t} \quad (4)$$

where COD₀ and COD_t were initial and final COD values after treatment time t (mg L⁻¹), F is Faraday's constant (96487 C mol⁻¹), I is the applied current (A), t is the electrolysis time (s), V is the volume of the solution (L), and 8 is the mass of oxygen present in the middle.

2.5. Box-Benhken experimental design.

The Box-Benhken design (BBD) is a mathematical model used to optimize experimental parameters generally used in the EF process [27,32]. BBD, a two-level mathematical model, is suitable for optimizing the process because the number of required tests is less than in other experimental designs. In this work, three main variables affecting the efficiency of TEN mineralization were chosen, corresponding to X1 for applied current I (mA), X2 for initial TEN concentration (mM), and X3 for electrolysis time t (min). The BB is a factorial plane represented on three levels: the high, low, and middle levels. Table 1 represents

the levels and the experimental range of independent variables for this work's optimization of TEN mineralization.

Table 1. Experimental level for COD removal of TEN for BBD.

Variables	Coded values	Level		
		- 1	0	+ 1
Applied Current, I(mA)	X ₁	200	300	400
Initial concentration of TEN, (mM)	X ₂	0.1	0.2	0.3
Time, t (min)	X ₃	60	120	180

Equation (5) was used to calculate the number of tests:

$$N = 2k \times (k - 1) + C \tag{5}$$

where N, k, and C correspond to the number of experiments, the number of independent variables, and the number of the central point, respectively [37]. It resulted in 15 tests to be carried out by using 3 central points. The response was the mineralization efficiency which was calculated as follows (Eq 6)

$$Y(\%) = \left(\frac{COD_0 - COD_t}{COD_0} \right) \times 100 \tag{6}$$

where COD₀ and COD_t correspond to the value of the organic chemical demand, respectively, at the initial time and time t.

The design of the different experiments and the analysis of the results were done by the MiniTAB 18 software. The experimental response associated with the BBD was characterized by a quadratic polynomial model (7):

$$Y = \beta_0 + \beta_1 X_1 + \beta_2 X_2 + \beta_3 X_3 + \beta_{11} X_1^2 + \beta_{22} X_2^2 + \beta_{33} X_3^2 + \beta_{12} X_1 X_2 + \beta_{13} X_1 X_3 + \beta_{23} X_2 X_3 + \beta_{123} X_1 X_2 X_3 + \varepsilon \tag{7}$$

where:

Y: is the predicted response, β_0 : the constant coefficient. β_i, β_{ij} : the coefficients of linear, interaction, and quadratic terms, respectively, X₃: coded variables ε : error term.

In order to assess the accuracy of the fitted model, the analysis of variance, the lack of fit, and the coefficient of determination R² were carefully exploited. After that, 3D graphs were plotted to show the response surface, the interaction between factors, and their combined effect on the efficiency of the treatment.

3. Results and discussion

3.1. Degradation of TEN.

3.1.1. Effect of applied current.

In order to study the kinetics of TEN degradations by the EF process, some electrolysis tests were investigated by varying the intensities of the current from 100 mA to 400 mA while maintaining the other parameters constant: initial pollutant concentration (0.3 mM), Fe²⁺ catalyst concentration (0.1 mM), pH = 3 and Na₂SO₄ (0.5 mM) at room temperature.

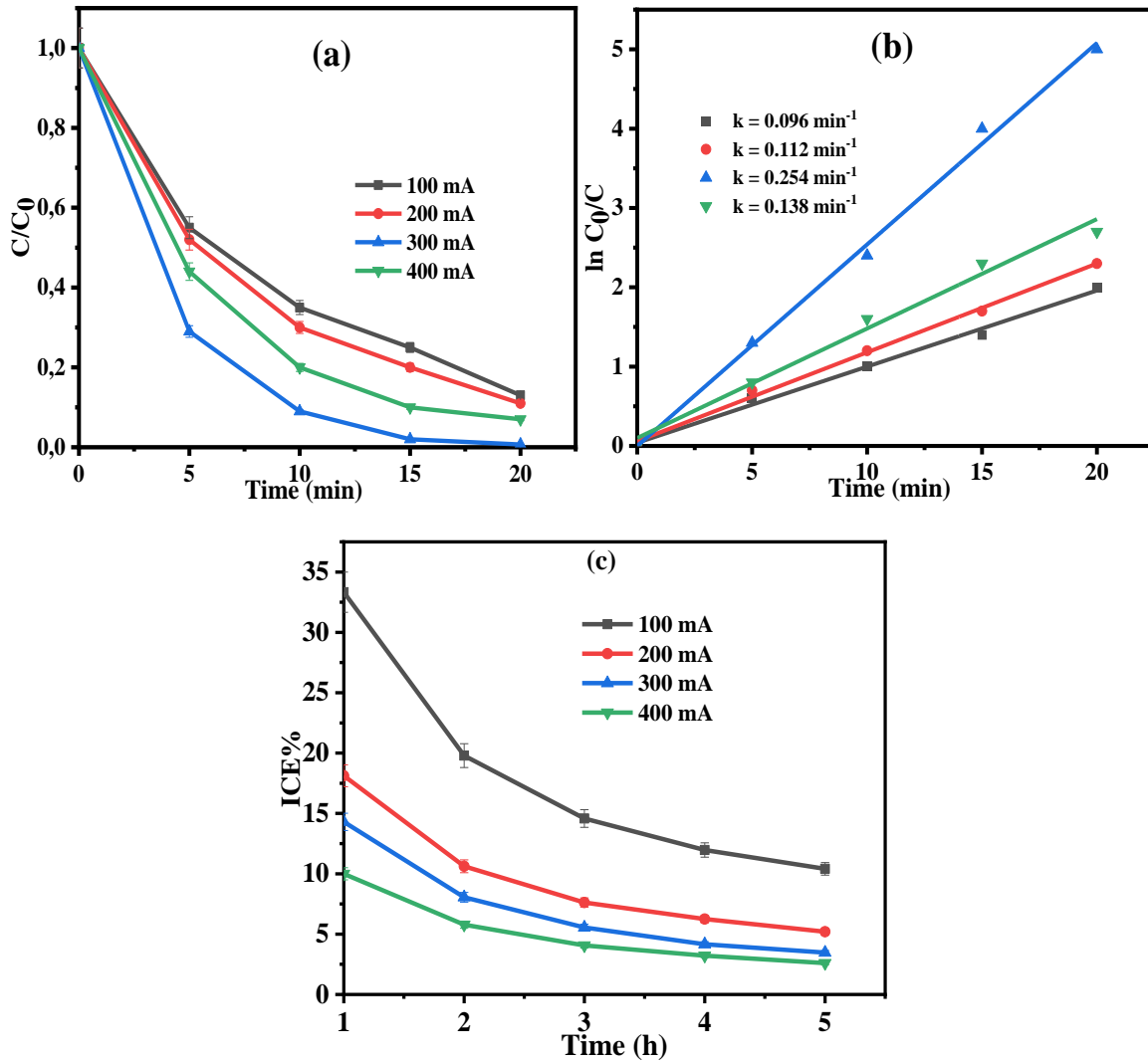
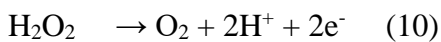
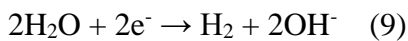
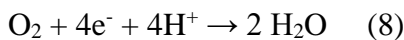


Figure 2. (a) Concentration decay of TEN during degradation by the E.F. process; (b) pseudo-first-order kinetic modeling; (c) ICE evolution with electrolysis time: V: 200 mL; [Fe²⁺] = 0.1 mM; [TEN] = 0.3 mM; [Na₂SO₄] = 0.5 M at room temperature.

From Figure 2a, it is observed that intensity has two distinct effects on TEN degradations. Firstly, the degradation efficiency was raised with the increase of the intensity from 100 (87.0%) to 300 (99.3%) mA, and secondly, a decrease to 400 mA (89.0%) was obtained. The increase in the rate of elimination of TEN is due to the augmentation reactions at the electrode, and more hydroxyl radicals were generated for TEN oxidation. Contrarily, the decrease in the degradation percentage of TEN at 400 mA is due to the overconsumption of electrical energy by secondary parasitic reactions that can take place at higher current intensities. Those reactions were the electrochemical reduction of O₂ (with the exchange of 4e⁻) leading to the formation of H₂O (Eq (8)), the increase in the formation of H₂ at the cathode (Eq (9)), and the oxidation of H₂O₂ at the anode (Eq (10)) [15,34,35].



To determine the constant rate, the equation of first order model rate (Eq 11) was applied for the case of TEN degradations by hydroxyl radicals (•OH) generated in the EF process.

$$\frac{d[\text{TEN}]}{dt} = k_{\text{app}}[\text{TEN}] \quad (11)$$

From Figure 2b, the exponential decrease in concentration during treatment clearly indicates the pseudo-first-order reaction kinetics ($R^2 > 0.99$) as reported in studies regarding applications EF process for organic pollutants degradation [34]. It can be seen that the exponential decay of the concentration of TEN increases linearly with increasing electrolysis time. The kinetic rate constants k_{app} obtained were 0.0989, 0.1157, 0.2540, and 0.1435 min^{-1} for 100, 200, 300, and 400 mA, respectively. The augmentation in k_{app} values from 0.0989 to 0.2540 min^{-1} is obviously due to the improvement of $\bullet\text{OH}$ production rate in the medium through the Fenton reaction.

The ICE is defined as the amount of charge used to mineralize the TEN throughout the electrolysis, was calculated. Figure 2c represents the results obtained. As shown in this figure, it appears the best ICE values are obtained at low current intensity. At $t = 60$ min, ICE% reaches 33.33% for $I = 100$ mA, followed by 18.12% for $I = 200$ mA. We also noted that ICE decreases with increasing the intensity of the current to 400 mA. This decrease explains mainly related to the disappearance of aromatic compounds and the formation of aliphatic and carboxylic compounds, which are endurance in the medium. Moreover, under these experimental conditions (high current and long electrolysis time), the two parasitic reactions (12) and (13) become dominant [17,36].



3.1.2. Effect of catalyst.

In the EP process, the initial concentration of the Fe^{2+} ions is a significant parameter affecting the treatment efficiency. In order to determine the effect of the catalyst quantity on the TEN degradation, the concentration of Fe^{2+} ions varied from 0.05 to 0.15 mM. The other parameters were kept constant as follows: initial TEN concentration ($C_0 = 0.3$ mM), pH (3), $I = 300$ mA, and Na_2SO_4 (0.5 mM) at room temperature.

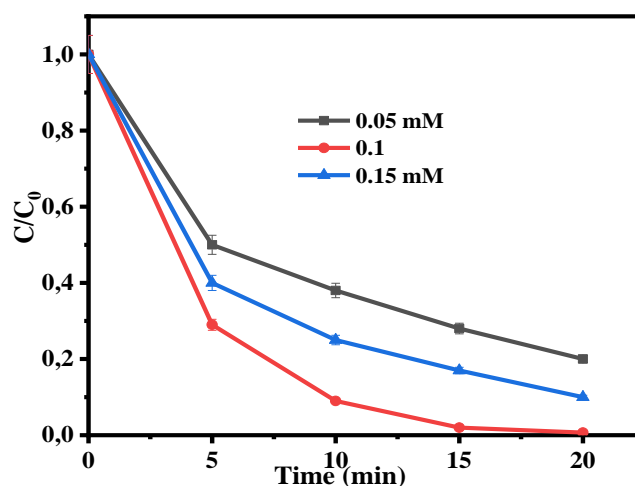


Figure 3. Effect of Fe^{2+} concentration during degradation of the TEN by E.F. process: $V: 200$ mL; $[\text{TEN}] = 0.3$ mM; $[\text{Na}_2\text{SO}_4] = 0.5$ M; $I = 300$ mA.

Figure 3 shows that the complete disappearance of TEN depends on the concentration of Fe^{2+} ions present in the medium. Indeed, the degradation percentages were 80.0, 99.3, and 90.0% for 0.05, 0.1, and 0.15 mM, respectively. Oxidation of TEN is, therefore, more effective for the concentration of 0.1 mM in Fe^{2+} compared to 0.05 and 0.15 mM. Similar observations have been reported in the literature [37–39]. The decrease in the rate of degradation of TEN

when the concentration of Fe^{2+} is above 0.1 mM can be explained by the parasitic reactions consuming hydroxyl radicals under excessive Fe^{2+} ions (14).



3.1.3 Effect of initial pollutant concentration.

Another parameter that can influence the degradation is the initial concentration of the pharmaceutical pollutant [44]. Therefore, we followed the treatment performed under the following experimental conditions: Fe^{2+} concentration (0.1 mM), current intensity (300 mA), and Na_2SO_4 (0.5 mM), while the initial concentration of the pollutant ranged from 0.1 to 0.3 mM under room temperature.

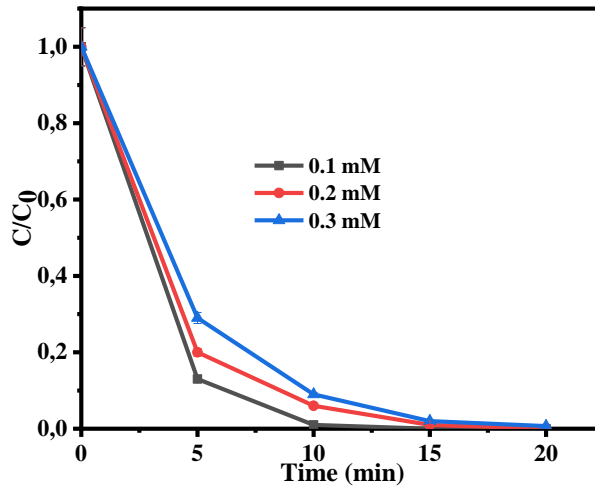


Figure 4. Influence of the initial concentration of TEN on degradation efficiency by the E.F. process. $[\text{Na}_2\text{SO}_4] = 0.5 \text{ M}$; $[\text{Fe}^{2+}] = 0.1 \text{ mM}$; $I = 300 \text{ mA}$

From Figure 4, it can be seen that the variation in the rate of degradation of TEN follows an exponential increase over time. We also noted that the degradation rate decreases with the increase in its initial concentration. Indeed, when the initial concentration increases from 0.1 to 0.3 mM, the degradation rate decreases from 100 to 91% after 10 minutes of electrolysis. This behavior is logically due to the rising target pollutants at higher concentrations, which are unfortunately more than the oxidative capacity of HO^\bullet radicals generated in the medium [45].

3.2 Biodegradability variation.

To achieve complete mineralization of antiviral drugs with EF process, there is a need for a long electrolysis time and high energy consumption simultaneously. Therefore, the combination of preliminary EF treatment to degrade the recalcitrant compounds with subsequent biodegradation is highly regarded as removing whole organic pollution at an affordable cost. In order to monitor the biodegradability of TEN solutions in this study, BOD5 measurements were carried out. The BOD5/COD represents the ratio allowing evaluation of the biodegradability of the solution during the treatment. As mentioned in the literature, to admit that the compound is biodegradable, this ratio must be higher than 0.33 [37,42].

The results obtained for biodegradability are represented in Figure 5. According to this figure, we can remark that the decrease in the COD of TEN favors the increase in BOD5/COD yield during the treatment time. Initially, the BOD5/COD yield of the TEN solutions was zero. It involves the slow decomposition of TEN in the environment, hence the interest in pretreating

before carrying out a biological treatment. Once the electrolysis was started, the BOD5/COD yield reached 0.1, 0.2, 9, and 11 after 2, 3, 4, and 5 h of treatment, respectively. Additionally, the COD values also increased from 92.8% to approximately 100% within 2-5 h electrolysis. This implies that after 2 h of treatment, the mineralization is increasingly weak; on the other hand, we have an increase in biodegradability as the application of the EF treatment progresses. Moreover, the biodegradability threshold would be about 3 h of electrolysis time because it is at this threshold that the treated solution can be considered biodegradable ($BOD_5/COD = 0.2$), which corresponds to almost complete mineralization (98%). The EF process used as a pretreatment step made it possible to transform the hardly biodegradable compounds into easily ingested ones by microorganisms that will provide plant nutrients [36,43,44]. These results show that the coupling between the two processes positively impacts research because it makes it possible to reduce economic costs (electrical energy).

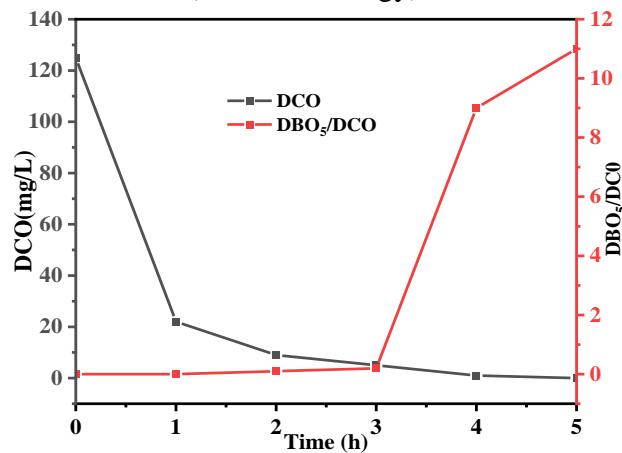


Figure 5. Variation of biodegradability during treatment of TEN. $I = 300 \text{ mA}$; $[Fe^{2+}] = 0.1 \text{ Mm}$; $[Na_2SO_4] = 0.5 \text{ M}$; $[TEN] = 0.3 \text{ mM}$.

3.3. Optimization of mineralization of TEN.

3.3.1. Influence of factors on mineralization of TEN.

The optimization of the mineralization of TEN was followed by RSM based on BBD. The influence of chosen factors (Current intensity, TEN Initial concentration, and treatment time) on DCO abatement was investigated while keeping Fe^{2+} concentration at 0.1 mM. The results are displayed in Figure 6 a-b.

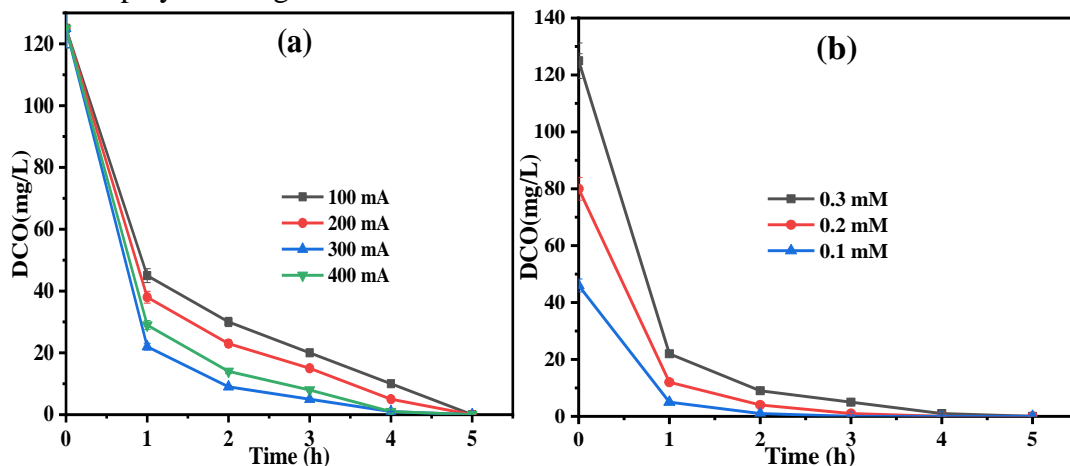


Figure 6. Influence of factors on mineralization of TEN by the EF process. (a) Current intensity; (b) initial TEN concentration. $[Na_2SO_4] = 0.5 \text{ M}$; $[Fe^{2+}] = 0.1 \text{ mM}$ V: 200 mL.

That value of Fe^{2+} concentration was chosen from a preliminary study of its influence on TEN mineralization, represented by Fig S1.

During the electrolysis time observed in Figure 6a, the COD decreases when the applied current increases from 100 to 300 mA. More than that value, increasing the intensity has no effect on the COD reduction. Indeed, after 4 h of electrolysis at applied currents of 100, 200, 300, and 400 mA, the mineralization percentages were 92.0%, 96.0%, 99.0%, and 99.0%, respectively. It is also noted that the reduction of the organic load is fast during the first hour of treatment and becomes slow for the longest durations of treatment. Generally, this phenomenon is noticed during the treatment of organic pollutants having aromatic nuclei by advanced oxidation processes (AOP) based on the in situ production of hydroxyl radicals $HO\bullet$. It is explained by the high reaction rate between aromatic compounds and $HO\bullet$ [43]. The rate of the mineralization reaction decreases with the electrolysis time due to: (i) the production of carboxylic acids and, in particular, of aliphatic compounds, which are difficult to oxidize by $HO\bullet$, (ii) high concentration of the pollutant leads to a drop the reaction rate during oxidation and (iii) competition between the secondary reactions produced in the medium and the $HO\bullet$ [49].

It is observed in Figure 6b that the electrolysis time required for total mineralization is a function of the concentration of TEN. The greater the initial concentration is, the longer the electrolysis time required for total mineralization. As observed in Figure 6a, the rate of mineralization, which increased at the start of the treatment, becomes progressively low for long durations of treatment. This phenomenon is explained by the fact that before the complete mineralization of the solution in CO_2 and H_2O , aliphatic intermediates are formed (carboxylic acids in particular), which do not react as quickly with the hydroxyl radicals $HO\bullet$. The efficiency of the EF process for TEN removals at different concentration ranges is well observed in Figure 6b. It can be deduced from these results that the EF process is a suitable method for the degradation of effluents loaded with medicinal products[45].

3.3.2. Box-Behnken design: statistical analysis.

Table 2 represents the different results obtained during our experimental matrix with the Box-Behnken (BBD) design to show the COD removal efficiency (response Y) by the EF process.

Table 2. Experimental and theoretical results for DCO removal.

Run N°	Variables			Response Y: DCO removal	
	X ₁ (mA)	X ₂ (mM)	X ₃ (min)	Y(observed)	Y (Predicted)
1	400	0.3	120	88.80	88.78
2	300	0.2	120	96.25	95.00
3	400	0.2	180	90.00	88.96
4	300	0.3	180	96.00	97.05
5	300	0.2	120	93.75	95.00
6	200	0.3	120	81.60	82.45
7	200	0.2	180	92.50	90.59
8	200	0.1	120	93.47	93.49
9	300	0.1	60	89.13	88.07
10	400	0.1	120	91.00	90.15
11	300	0.2	120	95.00	95.00
12	400	0.2	60	75.00	76.91
13	200	0.2	60	71.25	72.29
14	300	0.3	60	82.40	80.51
15	300	0.1	180	100.00	100.00

The data were analyzed by Mini-tab software, and the results were tested by analysis of variance for the TEN (Table 3).

Table 3. Results of analysis of variance for TEN removals.

Source	Sum of squares	Degrees of freedom	Mean square	F-value	p-value
Configuration	904.328	9	100.481	21.49	0.002
Residuals	542.215	3	180.738	38.65	0.001
Lack of Fit	20.254	3	6.751	4.32	0.194
Pure Error	3.125	2	1.563		
Error	23.379	5	4.676		
Total	927.707	14			

The high value of the F-test of the model (21.49) and the p-value of 0.002 indicate that the mathematical model interpreting the mineralization of TEN is statistically significant. In addition, the insignificant value (0.194) of lack of fit (LOF) means good adequacy of the model. The model's coefficient of determination (R^2) indicates that 97.48% of the total variability could be explained by the present quadratic polynomial model. The value of the adjusted coefficient of determination (adjusted $R^2 = 0.93$) also proved the accuracy of this model for the elimination of TEN. We will say as a conclusion guide that this model is valid to explain the answer Y. Thus, the predictive equation of this work will be interpreted. Then, the equation explaining the mineralization of TEN by EF process can be proposed as follow (Eq. (15)):

$$Y = 95.00 + 0.75 \cdot X_1 - 3.10 \cdot X_2 + 7.59 \cdot X_3 - 7.99 \cdot X_1 \cdot X_1 + 1.71 \cdot X_2 \cdot X_2 - 4.82 \cdot X_3 \cdot X_3 + 2.42 \cdot X_1 \cdot X_2 - 1.56 \cdot X_1 \cdot X_3 + 0.68 \cdot X_2 \cdot X_3 \quad (15)$$

The matching of the regression model could also be verified by plotting the experimental values versus the theoretical values calculated from the model equation. The graph depicted in Figure 7 revealed a good matching between these values with a straight correlation line. Thus, we can conclude that response Y perfectly represents the polynomial model.

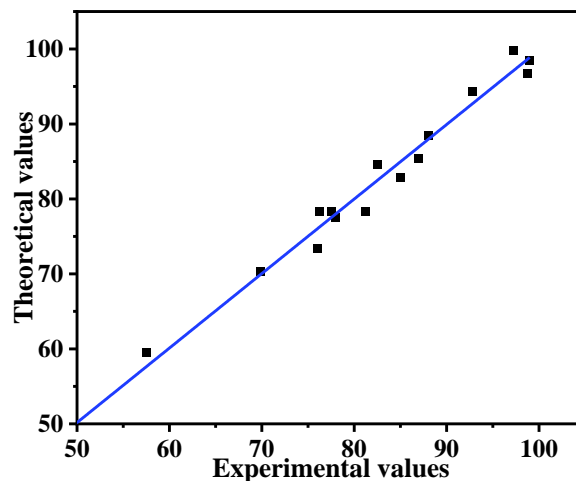


Figure 7. Correlation between experimental vs. theoretical values.

The coefficient of factor expressed in Eq. (11) exhibits the effect of each parameter on the mineralization of TEN. The factor having a positive coefficient directly increases the elimination of TEN, as shown, therefore, by the linear effect of the current (X_1) (mA) and electrolysis time (X_3) (min). Concerning interactions, the positive sign means that increasing both factors enhances mineralization efficiency. Regarding the negative effect of intensity-time

interaction, for example, it should be understood that the reverse variation of factors is rather favorable for removing TEN.

The 3D surface curve describing the evolution of the mineralization of TEN according to the interaction of current time, current-TEN concentration, and TEN concentration time is presented in Figure 8, Figure S2, and Figure S3, respectively.

According to Figure 8a, it can be seen that the augmentation of the current intensity from 200 to 300 mA when the electrolysis time increases from 60 to 180 minutes, the response Y also increases. Contrarily, the response decreases when the current rises from 300 to 400 mA. It is therefore deduced that the treatment efficiency increases with the intensity of the current. Therefore, it makes it possible to eliminate the TEN more quickly. Indeed, the maximum mineralization rate of the TEN is obtained when the current reaches 300 mA. This is due to the rapid formation of H₂O₂, thus favoring the high production of •OH. In addition, the electrolysis time also has a non-negligible effect on its mineralization because the electrolysis time is continuously linked to the intensity of the current. Both factors increase at the same time. We deduce that there is a strong interaction between both factors (intensity of the current and electrolysis time). In addition, the mineralization rate of TEN reaches the optimum condition.

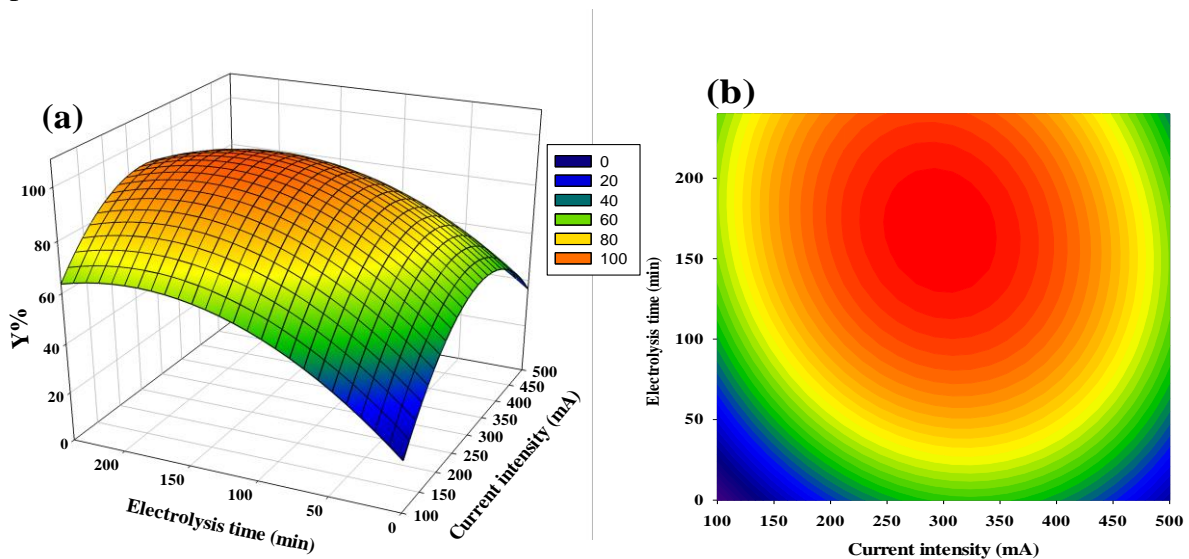


Figure 8. (a) Response surface curve for the interaction of intensity vs. electrolysis time; (b) Contour plot.

Figure 8b, which represents the contour plot between current intensity and electrolysis time, also corroborates the observations made on the response surface curve. The current intensity-electrolysis time interaction shows that the percentage of elimination is also a function of the increase in intensity and time of electrolysis.

The combination of these different investigations gave the following optimal condition for TEN mineralization (98%): current intensity 282 mA, 0.1 mM of TEN concentration for 164 min of treatment time.

4. Conclusions

The removal of TEN by the Electron-Fenton process was studied according to degradation and biodegradation efficiencies. TEN degradations (0.3 mM) by the E.F. process were obtained at a current intensity of 300 mA with a Fe²⁺ concentration of 0.1 mM after 20 min of electrolysis. The complementary of E.F. with further post-biodegradation was confirmed with biodegradation improvement (BOD₅/COD ratio of 0.2) after 3 h of treatment

for 0.3 mM of an initial TEN concentration. Also, the optimization of mineralization of TEN through RSM using Box-Benhen Design was used to obtain optimal conditions (current intensity 282 mA, 0.1 mM of TEN concentration for 164 min of time of treatment) required to eliminate the target pollutant. This study has revealed that coupling electrochemical treatment with biological degradation is a promising way to implement efficient and economical treatment processes to reduce drug contaminants in aqueous media.

Funding

This research received no external funding.

Acknowledgments

We thank all our colleagues.

Conflicts of Interest

The authors declare no conflict of interest.

References

1. Gwenzi, W.; Chaukura, N. Organic contaminants in African aquatic systems: Current knowledge, health risks, and future research directions. *Science of the Total Environment* **2018**, *619–620*, 1493–1514, <https://doi.org/10.1016/j.scitotenv.2017.11.121>.
2. Patel, M.; Kumar, R.; Kishor, K.; Mlsna, T.; Pittman, C. U.; Mohan, D. Pharmaceuticals of emerging concern in aquatic systems: Chemistry, occurrence, effects, and removal methods. *Chemical Reviews* **2019**, *119*, 3510–3673, <https://doi.org/10.1021/acs.chemrev.8b00299>.
3. Adeola, A. O.; Forbes, P. B. C. Antiretroviral Drugs in African Surface Waters: Prevalence, Analysis, and Potential Remediation. *Environmental Toxicology and Chemistry* **2022**, *41*, 247–262, <https://doi.org/10.1002/etc.5127>.
4. Babas, H.; Kaichouh, G.; Khachani, M.; Karbane, M. E.; Chakir, A.; Guenbour, A.; Bellaouchou, A.; Warad, I.; Zarrouk, A. Equilibrium and kinetic studies for removal of antiviral sofosbuvir from aqueous solution by adsorption on expanded perlite: Experimental, modelling and optimization. *Surfaces and Interfaces* **2021**, *23*, 100962, <https://doi.org/10.1016/j.surfin.2021.100962>.
5. Madikizela, L. M.; Ncube, S.; Chimuka, L. Analysis, occurrence and removal of pharmaceuticals in African water resources: A current status. *Journal of Environmental Management* **2020**, *253*, 109741, <https://doi.org/10.1016/j.jenvman.2019.109741>.
6. Shah, A. R. Electro-Fenton Oxidation of Simulated Pharmaceutical Waste: Optimization using Central Composite Design. *International Journal of Environmental Sciences & Natural Resources* **2017**, *3*, <https://doi.org/10.19080/ijesnr.2017.03.555623>.
7. Rodriguez-Nvoa, S.; Alvarez, E.; Labarga, P.; Soriano, V. Renal toxicity associated with tenofovir use. *Expert Opinion on Drug Safety* **2010**, *9*, 545–559, <https://doi.org/10.1517/14740331003627458>.
8. Onusida Statistiques mondiales sur le Vih en 2020. *Onusida* **2021**, *6*, <http://www.unaids.org/fr>.
9. Isnard-Bagnis, C.; Aloy, B.; Deray, G.; Turret, J. Tenofovir nephrotoxicity. *Nephrologie et Therapeutique* **2016**, *12*, 179–189, <https://doi.org/10.1016/j.nephro.2016.01.002>.
10. Hall, A. M.; Hendry, B. M.; Nitsch, D.; Connolly, J. O. Tenofovir-associated kidney toxicity in HIV-infected patients: A review of the evidence. *American Journal of Kidney Diseases* **2011**, *57*, 773–780, <https://doi.org/10.1053/j.ajkd.2011.01.022>.
11. Ncube, S.; Madikizela, L. M.; Chimuka, L.; Nindi, M. M. Environmental fate and ecotoxicological effects of antiretrovirals: A current global status and future perspectives. *Water Research* **2018**, *145*, 231–247, <https://doi.org/10.1016/j.watres.2018.08.017>.
12. Adeola, A. O.; Forbes, P. B. C. Assessment of reusable graphene wool adsorbent for the simultaneous removal of selected 2–6 ringed polycyclic aromatic hydrocarbons from aqueous solution. *Environmental Technology (United Kingdom)* **2022**, *43*, 1255–1268, <https://doi.org/10.1080/09593330.2020.1824024>.

13. Wood, T. P.; Duvenage, C. S. J.; Rohwer, E. The occurrence of anti-retroviral compounds used for HIV treatment in South African surface water. *Environmental Pollution* **2015**, *199*, 235–243, <https://doi.org/10.1016/j.envpol.2015.01.030>.
14. Al-Rajab, A. J.; Sabourin, L.; Chapman, R.; Lapen, D. R.; Topp, E. Fate of the antiretroviral drug tenofovir in agricultural soil. *Science of the Total Environment* **2010**, *408*, 5559–5564, <https://doi.org/10.1016/j.scitotenv.2010.07.074>.
15. Lou, W.; Kane, A.; Wolbert, D.; Rtimi, S.; Assadi, A. A. Study of a photocatalytic process for removal of antibiotics from wastewater in a falling film photoreactor: Scavenger study and process intensification feasibility. *Chemical Engineering and Processing: Process Intensification* **2017**, *122*, 213–221, <https://doi.org/10.1016/j.cep.2017.10.010>.
16. Kostich, M. S.; Batt, A. L.; Lazorchak, J. M. Concentrations of prioritized pharmaceuticals in effluents from 50 large wastewater treatment plants in the US and implications for risk estimation. *Environmental Pollution* **2014**, *184*, 354–359, <https://doi.org/10.1016/j.envpol.2013.09.013>.
17. Martínez-Huitle, C. A.; Brillas, E. Decontamination of wastewaters containing synthetic organic dyes by electrochemical methods: A general review. *Applied Catalysis B: Environmental* **2009**, *87*, 105–145, <https://doi.org/10.1016/j.apcatb.2008.09.017>.
18. El-Ghenymy, A.; Rodríguez, R. M.; Brillas, E.; Oturan, N.; Oturan, M. A. Electro-Fenton degradation of the antibiotic sulfanilamide with Pt/carbon-felt and BDD/carbon-felt cells. Kinetics, reaction intermediates, and toxicity assessment. *Environmental Science and Pollution Research* **2014**, *21*, 8368–8378, <https://doi.org/10.1007/s11356-014-2773-3>.
19. Wang, A.; Zhang, Y.; Han, S.; Guo, C.; Wen, Z.; Tian, X.; Li, J. Electro-Fenton oxidation of a β -lactam antibiotic cefoperazone: Mineralization, biodegradability and degradation mechanism. *Chemosphere* **2021**, *270*, 129486, <https://doi.org/10.1016/j.chemosphere.2020.129486>.
20. Ezzahra, F.; Zazou, H.; Afanga, H.; El, J.; Ait, R.; Veetil, P.; Hamdani, M. Journal of Water Process Engineering An overview on the elimination of organic contaminants from aqueous systems using electrochemical advanced oxidation processes. *Journal of Water Process Engineering* **2021**, *41*, 102040, <https://doi.org/10.1016/j.jwpe.2021.102040>.
21. Doumbi, R. T.; Bertrand Noumi, G.; Ngobtchok, B.; Domga Tannery wastewater treatment by electro-Fenton and electro-persulfate processes using graphite from used batteries as free-cost electrode materials. *Case Studies in Chemical and Environmental Engineering* **2022**, *5*, 100190, <https://doi.org/10.1016/j.csee.2022.100190>.
22. Oturan, M. A. Current Opinion in Solid State & Materials Science Outstanding performances of the BDD film anode in electro-Fenton process : Applications and comparative performance. *Current Opinion in Solid State & Materials Science* **2021**, *25*, 100925, <https://doi.org/10.1016/j.cossms.2021.100925>.
23. Wang, Z.; Liu, M.; Xiao, F.; Postole, G.; Zhao, H. Recent advances and trends of heterogeneous electro-Fenton process for wastewater treatment-review. *Chinese Chemical Letters* **2022**, *33*, 653–662, <https://doi.org/10.1016/j.ccl.2021.07.044>.
24. Martínez-pachón, D.; Echeverry-gallego, R. A.; Serna-galvis, E. A.; Miguel, J.; Botero-coy, A. M.; Hernández, F.; Torres-palma, R. A.; Moncayo-lasso, A. Science of the Total Environment Treatment of wastewater effluents from Bogotá – Colombia by the photo-electro-Fenton process : Elimination of bacteria and pharmaceutical. *Science of the Total Environment* **2021**, *772*, 144890, <https://doi.org/10.1016/j.scitotenv.2020.144890>.
25. Gopinath, A.; Pisharody, L.; Popat, A.; Nidheesh, P. V Current Opinion in Solid State & Materials Science Supported catalysts for heterogeneous electro-Fenton processes : Recent trends and future directions. *Current Opinion in Solid State & Materials Science* **2022**, *26*, 100981, <https://doi.org/10.1016/j.cossms.2022.100981>.
26. Akbal, F. Journal of Environmental Chemical Engineering Treatment of textile industry wastewater by electro-Fenton process using graphite electrodes in batch and continuous mode. **2021**, *9*, 104782, <https://doi.org/10.1016/j.jece.2020.104782>.
27. Mejjide, J.; Gómez, J.; Pazos, M.; Sanromán, M. A. Degradation of thiamethoxam by the synergetic effect between anodic oxidation and Fenton reactions. *Journal of Hazardous Materials* **2016**, *319*, 43–50, <https://doi.org/10.1016/j.jhazmat.2016.02.064>.
28. heidari, M.; Vosoughi, M.; Sadeghi, H.; Dargahi, A.; Mokhtari, S. A. Degradation of diazinon from aqueous solutions by electro-Fenton process: effect of operating parameters, intermediate identification, degradation pathway, and optimization using response surface methodology (RSM). *Separation Science and Technology (Philadelphia)* **2021**, *56*, 2287–2299, <https://doi.org/10.1080/01496395.2020.1821060>.

29. Shokoohi, R.; Nematollahi, D.; Reza, M. Environmental Technology & Innovation Optimization of three-dimensional electrochemical process for degradation of methylene blue from aqueous environments using central composite design. *Environmental Technology & Innovation* **2020**, *18*, 100711, <https://doi.org/10.1016/j.eti.2020.100711>.
30. Basturk, I.; Varank, G.; Murat Hocaoglu, S.; Yazici Guvenc, S. Medical laboratory wastewater treatment by electro-fenton process: Modeling and optimization using central composite design. *Water Environment Research* **2021**, *93*, 393–408, <https://doi.org/10.1002/wer.1433>.
31. Zhu, X.; Tian, J.; Liu, R.; Chen, L. Optimization of fenton and electro-fenton oxidation of biologically treated coking wastewater using response surface methodology. *Separation and Purification Technology* **2011**, *81*, 444–450, <https://doi.org/10.1016/j.seppur.2011.08.023>.
32. Rachidi, L.; Kaichouh, G.; Khachani, M.; Zarrouk, A.; Karbane, M. El; Chakchak, H.; Warad, I.; Hourch, A. EL; Kacemi, K. El; Guessous, A. Optimization and modeling of the electro-Fenton process for treatment of sertraline hydrochloride: Mineralization efficiency, energy cost and biodegradability enhancement. *Chemical Data Collections* **2021**, *35*, 100764, <https://doi.org/10.1016/j.cdc.2021.100764>.
33. Ferrag-Siagh, F.; Fourcade, F.; Soutrel, I.; Aït-Amar, H.; Djelal, H.; Amrane, A. Tetracycline degradation and mineralization by the coupling of an electro-Fenton pretreatment and a biological process. *Journal of Chemical Technology and Biotechnology* **2013**, *88*, 1380–1386, <https://doi.org/10.1002/jctb.3990>.
34. Mansour, D.; Fourcade, F.; Soutrel, I.; Hauchard, D.; Bellakhal, N.; Amrane, A. Mineralization of synthetic and industrial pharmaceutical effluent containing trimethoprim by combining electro-Fenton and activated sludge treatment. *Journal of the Taiwan Institute of Chemical Engineers* **2015**, *53*, 58–67, <https://doi.org/10.1016/j.jtice.2015.02.022>.
35. Aboudalle, A.; Djelal, H.; Domergue, L.; Fourcade, F.; Amrane, A. A novel system coupling an electro-Fenton process and an advanced biological process to remove a pharmaceutical compound, metronidazole. *Journal of Hazardous Materials* **2021**, *415*, 125705, <https://doi.org/10.1016/j.jhazmat.2021.125705>.
36. Puga, A.; Moreira, M. M.; Figueiredo, S. A.; Delerue-Matos, C.; Pazos, M.; Rosales, E.; Sanromán, M. Á. Electro-Fenton degradation of a ternary pharmaceutical mixture and its application in the regeneration of spent biochar. *Journal of Electroanalytical Chemistry* **2021**, *886*, 115135, <https://doi.org/10.1016/j.jelechem.2021.115135>.
37. Hassani, A.; Eghbali, P.; Kakavandi, B.; Lin, K. A. Environmental Technology & Innovation Acetaminophen removal from aqueous solutions through nanocomposite: Insight into the performance and degradation kinetics. *Environmental Technology & Innovation* **2020**, *20*, 101127, <https://doi.org/10.1016/j.eti.2020.101127>.
38. Ghanbari, F.; Hassani, A.; Waclawek, S.; Wang, Z.; Matyszczyk, G.; Lin, K. Y. A.; Dolatabadi, M. Insights into paracetamol degradation in aqueous solutions by ultrasound-assisted heterogeneous electro-Fenton process: Key operating parameters, mineralization and toxicity assessment. *Separation and Purification Technology* **2021**, *266*, <https://doi.org/10.1016/j.seppur.2021.118533>.
39. Gholizadeh, A. M.; Zarei, M.; Ebratkhahan, M.; Hasanzadeh, A. Phenazopyridine degradation by electro-Fenton process with magnetite nanoparticles-activated carbon cathode, artificial neural networks modeling. *Journal of Environmental Chemical Engineering* **2021**, *9*, 104999, <https://doi.org/10.1016/j.jece.2020.104999>.
40. Arhoutane, M. R.; Yahya, M. S.; El Karbane, M.; Guessous, A.; Chakchak, H.; El Kacemi, K. Removal of pyrazinamide and its by-products from water: Treatment by electro-Fenton process and feasibility of a biological post-treatment. *Mediterranean Journal of Chemistry* **2019**, *8*, 53–65, <https://doi.org/10.13171/mjc811903420mra>.
41. Ganzenko, O.; Trellu, C.; Oturan, N.; Huguenot, D.; Péchaud, Y.; van Hullebusch, E. D.; Oturan, M. A. Electro-Fenton treatment of a complex pharmaceutical mixture: Mineralization efficiency and biodegradability enhancement. *Chemosphere* **2020**, *253*, 126659, <https://doi.org/10.1016/j.chemosphere.2020.126659>.
42. Yang, W.; Zhou, M.; Oturan, N.; Li, Y.; Oturan, M. A. Electrocatalytic destruction of pharmaceutical imatinib by electro-Fenton process with graphene-based cathode. *Electrochimica Acta* **2019**, *305*, 285–294, <https://doi.org/10.1016/j.electacta.2019.03.067>.
43. Yahya, M. S.; Beqqal, N.; Guessous, A.; Arhoutane, M. R.; El Kacemi, K. Degradation and mineralization of moxifloxacin antibiotic in aqueous medium by electro-Fenton process: Kinetic assessment and oxidation products. *Cogent Chemistry* **2017**, *3*, 1290021, <https://doi.org/10.1080/23312009.2017.1290021>.
44. Ma, H.; Yu, B.; Wang, Q.; Owens, G.; Chen, Z. Enhanced removal of pefloxacin from aqueous solution by

- adsorption and Fenton-like oxidation using NH₂-MIL-88B. *Journal of Colloid and Interface Science* **2021** , 583, 279–287, <https://doi.org/10.1016/j.jcis.2020.09.034>.
45. Görmez, Ö.; Akay, S.; Gözmen, B.; Kayan, B.; Kalderis, D. Degradation of emerging contaminant coumarin based on anodic oxidation, electro-Fenton and subcritical water oxidation processes. *Environmental Research* **2022** , 208, 112736, <https://doi.org/10.1016/j.envres.2022.112736>.
46. Oller, I.; Malato, S.; Sánchez-Pérez, J. A. Combination of Advanced Oxidation Processes and biological treatments for wastewater decontamination-A review. *Science of the Total Environment* **2011**, 409, 4141–4166, <https://doi.org/10.1016/j.scitotenv.2010.08.061>.
47. Olvera-Vargas, H.; Cocerva, T.; Oturan, N.; Buisson, D.; Oturan, M. A. Bioelectro-Fenton: A sustainable integrated process for removal of organic pollutants from water: Application to mineralization of metoprolol. *Journal of Hazardous Materials* **2016** , 319, 13–23, <https://doi.org/10.1016/j.jhazmat.2015.12.010>.
48. Aboudalle, A.; Djelal, H.; Domergue, L.; Fourcade, F.; Amrane, A.; Unilasalle-ecole, M. A novel system coupling an electro-Fenton process and an advanced biological process to remove a pharmaceutical compound , metronidazole. *Journal of Hazardous Materials* **2021**, 415, 125705, <https://doi.org/10.1016/j.jhazmat.2021.125705>.
49. Rezgui, S.; Ghazouani, M.; Bousselmi, L.; Akrou, H. Efficient treatment for tannery wastewater through sequential electro-Fenton and electrocoagulation processes. *Journal of Environmental Chemical Engineering* **2022**, 10, 107424, <https://doi.org/10.1016/j.jece.2022.107424>.

Supplementary materials

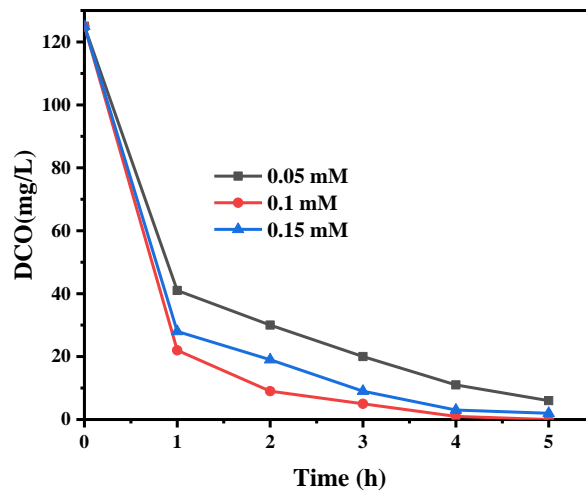


Figure S1. Influence of the concentration of the Fe²⁺ catalyst on mineralization by the E.F process. V: 200 mL; [Na₂SO₄] = 0.5 M; [TEN] = 0.3 mM; I= 300 mA.

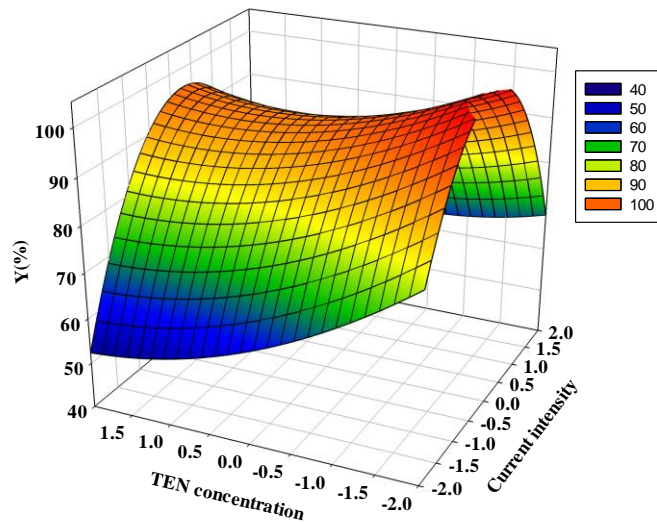


Figure S2. (a) Response surface curve for interaction of intensity vs. TEN concentration; (b) Contour plot.

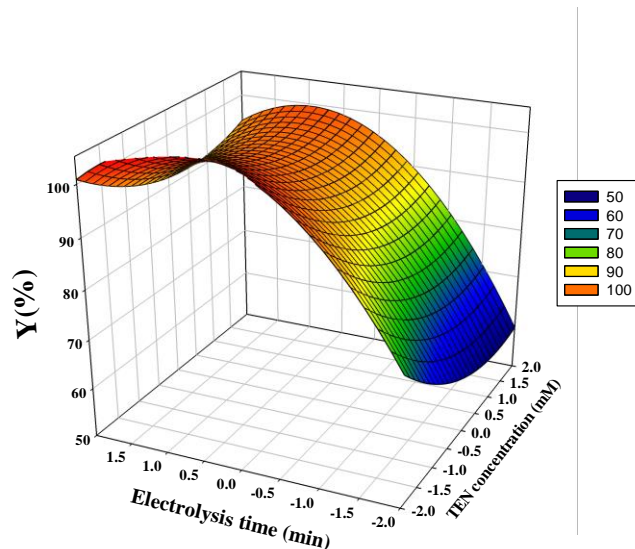


Figure S3. (a) Response surface curve for interaction of intensity vs. TEN concentration; (b) Contour plot.